RNA (1998), *4*:1096–1110. Cambridge University Press. Printed in the USA.

Intronic snoRNA biosynthesis in *Saccharomyces cerevisiae* depends on the lariat-debranching enzyme: Intron length effects and activity of a precursor snoRNA

SIEW LOON OOI,[1] DMITRY A. SAMARSKY,[2,3] MAURILLE J. FOURNIER,[2] and JEF D. BOEKE[1]

[1]Department of Molecular Biology and Genetics, Johns Hopkins University School of Medicine, Baltimore, Maryland 21205, USA
[2]Department of Biochemistry and Molecular Biology, University of Massachusetts, Amherst, Massachusetts 01003, USA

ABSTRACT

The eukaryotic small nucleolar RNAs (snoRNAs) are involved in processing of pre-rRNA and modification of rRNA nucleotides. Some snoRNAs are derived from mono- or polycistronic transcription units, whereas others are encoded in introns of protein genes. The present study addresses the role of the RNA lariat-debranching enzyme (Dbr1p) in the synthesis and function of intronic snoRNAs in the yeast *Saccharomyces cerevisiae*. Intronic snoRNA production was determined to depend on Dbr1p. Accumulation of mature intronic snoRNAs is reduced in a *dbr1* mutant; instead, intronic snoRNAs are "trapped" within host intron lariats. Interestingly, the extent of intronic snoRNA accumulation in the form of lariats in *dbr1* cells varied among different intronic snoRNAs. Intronic snoRNAs encoded within shorter introns, such as U24 and snR38, accumulate more unprocessed lariat precursors than those encoded within longer introns, e.g., U18 and snR39. This correlation was corroborated by experiments conducted with model intron:U24 snoRNA constructs. These results support a splicing-dependent exonucleolytic pathway for the biosynthesis of intronic snoRNAs. Curiously, U24 in a lariat may be functional in directing methylation of ribosomal RNA.

Keywords: *DBR1*; intronic snoRNA processing; rRNA methylation; yeast

INTRODUCTION

Eukaryotic cells contain scores of metabolically stable small RNAs in the nucleolus that function in ribosome biogenesis (reviewed in Maxwell & Fournier, 1995; Bachellerie & Cavaille, 1997; Smith & Steitz, 1997; Tollervey & Kiss, 1997). A few of these small nucleolar RNAs (snoRNAs) are involved in cleavage events that process precursor ribosomal RNA into mature 18S, 5.8S, and 25S/28S species. Most, and perhaps all, are predicted to direct site-specific pseudouridylation and 2′-*O*-methylation of rRNA.

All snoRNAs, except one (MRP RNA), can be classified into two families based on short consensus sequences: the box C/D and box H/ACA snoRNAs (reviewed in Balakin et al., 1996; Ganot et al., 1997b; Smith & Steitz, 1997; Tollervey & Kiss, 1997). The box C/D snoRNAs are distinguished by sequence elements known as box C and box D, which are usually located at the 5′ and 3′ ends of the mature RNA, respectively (Fig. 1A). Boxes C and D are brought together in the folded pre-snoRNA, in most cases by formation of an adjoining stem(s), to form a structural motif known as the box C/D motif. This motif is required for processing, stability, and localization of the snoRNA to the nucleolus (Samarksy et al., 1998 and references therein). Most box C/D snoRNAs contain a second set of box C and D elements located in the interior, and these are designated boxes C′ and D′, respectively (Kiss-Laszlo et al., 1998; D.A. Samarsky, unpubl.). Nearly all box C/D snoRNAs known or predicted also contain one or two long sequences complementary to rRNA, which immediately precede the box D or D′ element. These snoRNAs interact transiently with the corresponding rRNA segments and guide the formation of 2′-*O*-

Reprint requests to: Jef D. Boeke, Department of Molecular Biology and Genetics, Johns Hopkins University School of Medicine, 725 N. Wolfe Street, 617 Hunterian Building, Baltimore, Maryland 21205, USA; e-mail: jef_boeke@qmail.bs.jhu.edu.
[3]Present address: Program in Molecular Medicine, University of Massachusetts Medical Center, Worcester, Massachusetts 01605, USA.

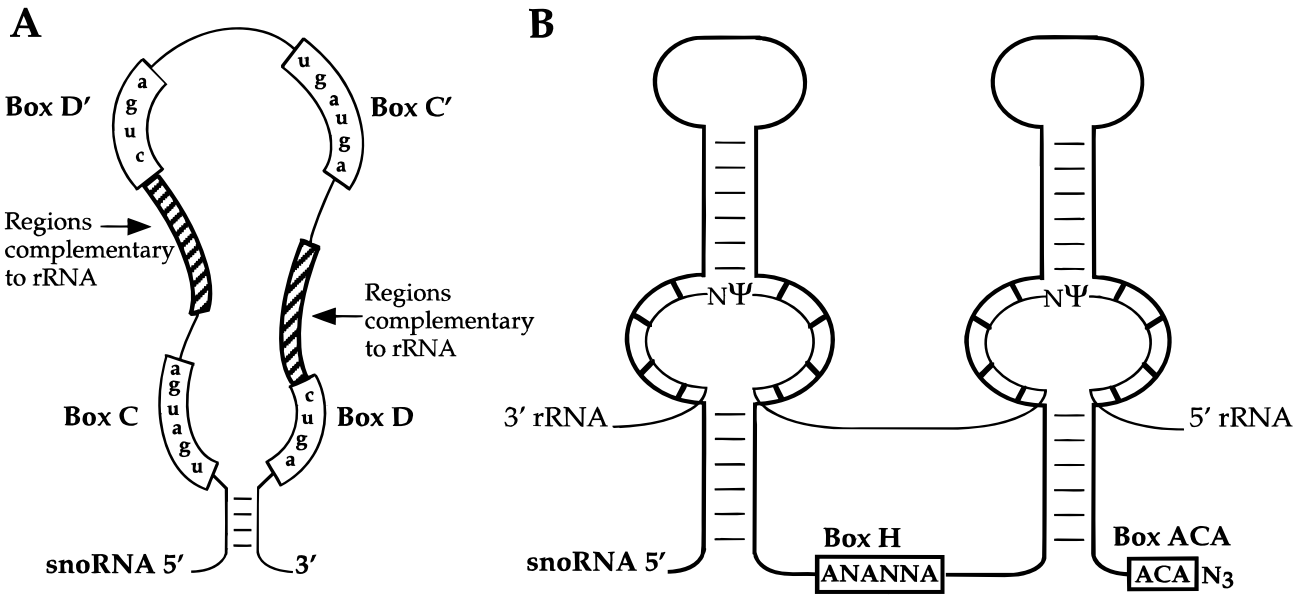

FIGURE 1. Schematic structure of box C/D and box H/ACA snoRNAs (adapted from Tollervey & Kiss, 1997). **A:** Box C/D snoRNAs are distinguished by two sequence elements, box C and box D. Boxes C and D are brought together in the folded pre-snoRNA and form a structure known as the box C/D motif, which is required and sufficient for RNA processing, stability, and nucleolar localization (see text). The middle region of some snoRNAs contains a second set of box C and box D sequences, designated boxes C′ and D′, respectively. In most box C/D snoRNAs, regions complementary to rRNA are located upstream of box D or D′ (indicated by hatched boxes). In conjunction with box D or D′, these antisense sequences target rRNA nucleotides for 2′-*O*-methylation. **B:** Box H/ACA snoRNAs contain box H, located in the "hinge" region of the snoRNA, and box ACA, a trinucleotide element located three nucleotides upstream of the 3′ end (see text). Both box elements are required for snoRNA production. A consensus secondary structure contains stem-loop domains near the 5′ and 3′ ends. One or both of these boxes contain short regions complementary to rRNA, which target pseudouridine synthesis in rRNA (Ψ). Box elements in both classes of snoRNAs are predicted to form protein recognition signals.

methylated nucleotides, at a precise distance from box D or D′ (Cavaille et al., 1996; Kiss-Laszlo et al., 1996; Tycowski et al., 1996b). The box H/ACA snoRNAs contain box H, located in a consensus "hinge" region of the molecule, and box ACA, a trinucleotide element located upstream of the 3′ end (Fig. 1B). These elements are also required for snoRNA production (Balakin et al., 1996; Ganot et al., 1997b). At least 15 box H/ACA snoRNAs are known to direct site-specific pseudouridylation of rRNA, suggesting that most snoRNAs in this family have this function (Ganot et al., 1997a; Ni et al., 1997). As with snoRNA-mediated methylation, selection of the target rRNA nucleotide involves direct base pairing of the snoRNA and rRNA, and modification of a nucleotide located at a fixed distance from a box H or box ACA element.

In addition to possessing unique function, snoRNAs exhibit unusual patterns of synthesis. Some of them are derived from mono- or polycistronic snoRNA transcription units, whereas many are encoded within introns of protein genes; most mammalian snoRNAs known are intronic (Leader et al., 1994, 1997; Maxwell & Fournier, 1995). The intronic snoRNAs are usually encoded within genes that specify proteins involved in ribosome synthesis or function, although some are specified by genes that give rise to untranslatable spliced exons (Tycowski et al., 1996a; Bortolin & Kiss, 1998). The general mechanism of intronic snoRNA production is still not clear. Results from studies with the box C/D U16 and U18 snoRNAs in *Xenopus* oocytes suggest a splicing-independent pathway, involving endonucleolytic cleavage of the snoRNA-containing pre-mRNA transcript (Fragapane et al., 1993; Prislei et al., 1993; Caffarelli et al., 1994, 1996; Prislei et al., 1995). Studies with the box H/ACA U19 snoRNA in vitro and box H/ACA U17 snoRNA both in vitro and in *Xenopus* oocytes argue against the participation of endonucleases, consistent with a splicing-dependent pathway for snoRNA production (Cecconi et al., 1995; Kiss & Filipowicz, 1995). Maturation results obtained with experimental box C/D U14 snoRNAs in *Xenopus* oocytes and the box C/D U20 snoRNA in cultured mouse cells favor the splicing-dependent pathway, but do not exclude a splicing-independent scheme (Cavaille & Bachellerie, 1996; Watkins et al., 1996).

According to a splicing-dependent model, the pre-mRNA–snoRNA transcript moves through the normal splicing pathway and the first snoRNA processing step is the formation of spliced exons and a snoRNA-containing intron lariat. The covalent bond at the lariat branch point is then hydrolyzed by the RNA lariat-debranching enzyme and the linearized product is subsequently trimmed at both ends by exonucleases. If an intron does not contain a snoRNA, the debranched lar-

iat is completely degraded by exonucleases. However, if an intron contains a box C/D or box H/ACA snoRNA, the snoRNA segment will be protected from complete degradation, presumably through binding of hypothetical proteins to the box C/D or box H/ACA structural motifs (see also Watkins et al., 1996; Ganot et al., 1997b).

In a recent study, synthesis of intronic snoRNAs in *Saccharomyces cerevisiae* was shown to depend on the RNA lariat-debranching enzyme Dbr1p (Petfalski et al., 1998). Previous characterization of a *dbr1* strain revealed that introns accumulate to very high levels in mutant cells, and that intron lariats are present in the form of "nibbled" lariats, missing the linear sequences on the 3′ side of the branch point (Chapman & Boeke, 1991). In the snoRNA study, the intronic box C/D snoRNA U24 was found to accumulate almost exclusively as a larger precursor in *dbr1* mutants, with electrophoretic mobility characteristic of intron lariats (Chapman & Boeke, 1991; Petfalski et al., 1998). This observation argues that intronic snoRNA production in yeast occurs by a splicing-dependent pathway. Paradoxically, a different pattern was observed for another intronic box C/D snoRNA examined in this study. U18 accumulated in both lariat and mature RNA forms at comparable levels, consistent with an alternative, splicing-independent pathway.

With a view to further defining the relationship between intronic snoRNA biogenesis and splicing, we analyzed production of more than 15 different small nucleolar RNAs in the yeast *dbr1* mutant, encoded in both natural and nonnatural genomic contexts. Particular emphasis was made on establishing the nature of events leading to Dbr1p-independent release of intronic snoRNAs from the intron lariat "trap" (see above). Another major issue addressed in our study is whether a snoRNA trapped in the lariat retains its biological activity. This was done by comparing individual rRNA methylation patterns in wild-type and *dbr1* mutant cells.

RESULTS

Intronic snoRNA biosynthesis depends on debranching enzyme

To determine the importance of the Dbr1p for snoRNA production, we examined expression of all known intronic and several nonintronic snoRNAs in *S. cerevisiae dbr1* mutant cells. In particular, we used the *dbr1* mutant, KC99, which is viable and has the *DBR1* coding region disrupted by the *HIS3* marker gene (Chapman & Boeke, 1991). In *dbr1* cells, introns accumulate in the form of lariats missing the linear sequences on the 3′ side of the branch point (Chapman & Boeke, 1991). This is readily observed on a total RNA blot fractionated on a polyacrylamide gel, because the mobility of the lariat form differs from that of linear RNA molecules of the same size (Chapman & Boeke, 1991).

Blot analysis of total RNA showed that in both wild-type and *dbr1* cells, the nonintronic snoRNAs accumulate exclusively in the mature form (Fig. 2A). The species examined included the box C/D snoRNAs snR13, U3b, U14, snR4, snR45, and snR190 and the box H/ACA snoRNA snR35. In contrast, the intronic box C/D snoRNAs snR39, snR59, U24, snR38, and U18, and the intronic box H/ACA snoRNA snR44 all accumulate in both unprocessed (top band) and mature (bottom band) forms in the *dbr1* cells (Fig. 2B).

To verify that the unprocessed, slowest migrating band on the gel corresponds to an intron lariat with a 2′-5′ phosphodiester linkage at the branch point, total RNA from *dbr1* cells was treated with recombinant His-tagged Dbr1p enzyme and examined by total RNA blotting (Fig. 2C; see also Nam et al., 1994, 1997). The radiolabeled oligonucleotide used to probe the blot specifically recognizes the intronic U24 snoRNA. The RNA pattern obtained demonstrates that the increase in debranching enzyme concentration results in a shift from the slowest to the second-slowest migrating band (Fig. 2C, lanes 3–5). This result confirms that the slowest migrating band corresponds to an unprocessed intron lariat. It also provides an independent indication that the second band observed for some RNAs corresponds to a linearized intron (e.g., U24 and snR38, Fig. 2B). This second band has the appropriate electrophoretic mobility (compare lanes 2 and 3–5 in Fig. 2C), and it hybridizes with probes specific to the snoRNA itself, as well as to intron segments both upstream and downstream of the snoRNA coding region (data for snR38 are shown in Fig. 2D; data for U24 are not shown). The presence of the linearized intron species on the blots is believed to be an artifact that occurs during RNA extraction and has been observed previously (Nam et al., 1997). Linearized intron can result either from specific breakage of the 2′-5′ phosphodiester bond at the branch point or of any 3′-5′ phosphodiester bond within the lariat. Because the intron lariat lacks a 3′ extension, these two species have identical length and therefore identical electrophoretic mobility.

Upon longer exposure of the film, a third band migrating faster than the linearized intron can be observed on total RNA blots from *dbr1* cells probed for U24, snR38, and U18. A longer exposure of the autoradiogram from such a blot hybridized with the snR38 probe is shown in Figure 2D (lanes 1 and 2). The third-slowest migrating band appears to correspond to 5′-extended pre-snoRNA because it hybridizes to probes specific to the intron segment upstream but not downstream of the snR38 coding region (Fig. 2D; lanes 4 and 5 versus 7 and 8). Similar results were obtained with U24 snoRNA (data not shown). The significance of the 5′-extended pre-snoRNA will be addressed in the Discussion.

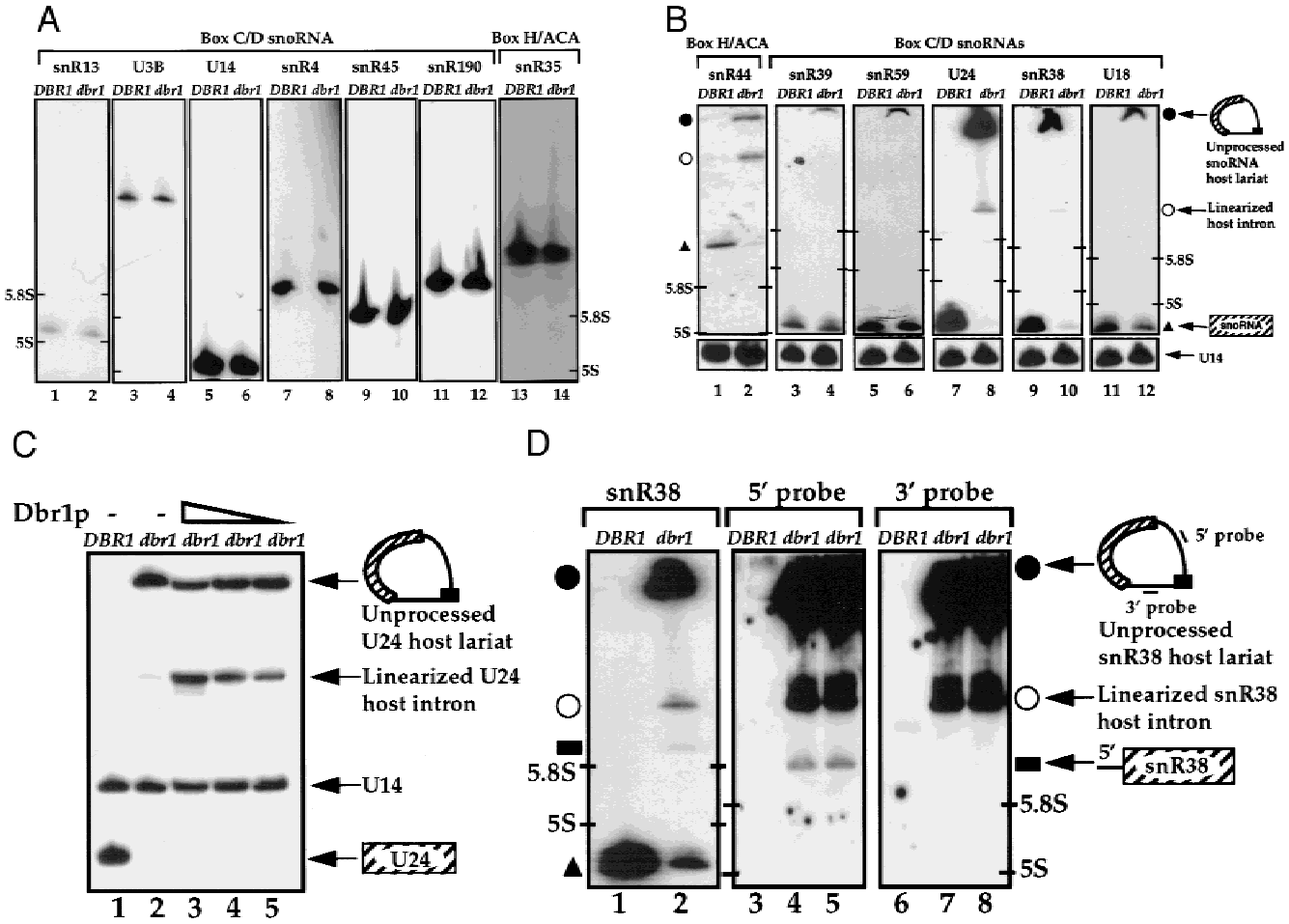

FIGURE 2. Analysis of nonintronic and intronic snoRNA production in a *dbr1* mutant. **A:** Nonintronic snoRNA species. **B:** Intronic snoRNA species. Total RNA was isolated from *S. cerevisiae* wild-type *DBR1* (strain YH8) and mutant *dbr1* (strain KC99) cells. Ten micrograms (Fig. 2A, all lanes; Fig. 2B, lanes 3–12) or 30 μg (Fig. 2B, lanes 1–2) of total RNA was fractionated on a denaturing polyacrylamide gel. Polyacrylamide gel concentrations used were 10% (panel A, lanes 1–2; panel B, lanes 3–12), 8% (panel A, lanes 3–14) or 5% (panel B, lanes 1–2). Oligonucleotide probes used are described in Table 2. Analysis of snR59, U24, snR38, and U18 (panel B, lanes 5–12) was performed by sequentially re-probing the same blot (stripped prior to re-probing). All figures were cropped at the gel wells. **C:** Treatment of *dbr1* total RNA with recombinant His-tagged Dbr1p enzyme. Total RNA was isolated from *DBR1* (strain YH8, lane 1) and *dbr1* (strain KC99, lanes 2–5) strains. Ten micrograms of total RNA from *dbr1* cells was then treated with 0 ng (lane 2), 465 ng (lane 3), 140 ng (lane 4), or 46 ng (lane 5) of recombinant His-tagged Dbr1p protein as described in Materials and Methods. Hybridization analysis was performed with a U24-specific probe. **D:** Analysis of pre-snR38 5′- and 3′-extended regions. Lanes 1 and 2 show the longer exposure version of the snR38 total RNA blot shown in panel B, lanes 9 and 10. Total RNA was isolated from *S. cerevisiae DBR1* (strain YH8, lanes 3 and 6) and *dbr1* (strain KC99, lanes 4 and 7; strain KC106, lanes 5 and 8) cells. Hybridization analysis was performed as described in Materials and Methods with equal amounts of total RNA loaded in each lane, using probes specific to the snR38 intron 5′ region (JB1694, lanes 3–5) or 3′ region (JB1695, lanes 6–8). Blot was exposed to X-ray film for 7 days at −70 °C. In panels B, C, and D, unprocessed lariat, linearized, 5′-extended, and mature intronic snoRNA forms are marked with a filled circle, open circle, filled rectangle, and filled triangle, respectively; the symbols on the right depict these snoRNA forms. Unprocessed snoRNA trapped in the lariat form is depicted by a hatched arc; a filled rectangle represents the branch point; mature snoRNA is depicted by a hatched box. Position of 5.8S (~160 nt) and 5S (~120 nt) rRNAs are indicated. GenBank accession numbers for the following snoRNAs are given in the parentheses: snR13 (U16692); U3B (X05498, the gene name is snR17B); U14 (X96815); snR4 (U57010); snR45 (U56646); snR190 (X96815); snR35 (L33803); snR44 (U56645); snR39 (U26011); snR59 (AF064271); U24 (Z48760); snR38 (U26012); and U18 (U12981).

Heterologous *DBR1* genes and intronic snoRNA biosynthesis

It was shown previously that *DBR1* gene homologues from the yeast *Schizosaccharomyces pombe* and the nematode *Caenorhabditis elegans* can complement the intron accumulation defect in *S. cerevisiae dbr1* cells (Nam et al., 1997). Here, we asked whether heterologous *DBR1* can also complement the defect in intronic snoRNA synthesis in *dbr1* cells. *S. pombe dbr1*$^+$ and *C. elegans dbr-1*(+) cDNAs fused to the *GAL1* promoter were introduced on centromeric plasmids bearing *TRP1* and *URA3* markers, respectively, into *S. cerevisiae dbr1* cells. Analysis of U24 RNA accumula-

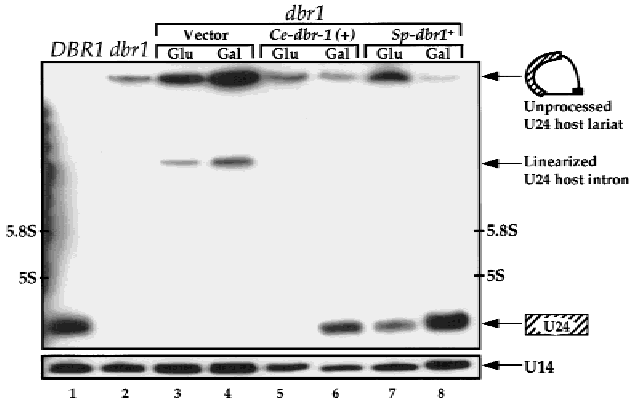

FIGURE 3. Complementation of the U24 biosynthesis defect in *dbr1* cells by heterologous *DBR1* genes. RNA analyzed was isolated from: *DBR1* (strain YH8, lane 1), *dbr1* (strain KC99, lane 2), *dbr1* transformed with vector pRS314GU alone (strain YSO1, lanes 3 and 4), *dbr1* transformed with plasmid expressing *C. elegans dbr-1*$^+$ cDNA fused to the *GAL1* promoter on plasmid pRS314GU (strain YKN120, lanes 5 and 6), and *dbr1* transformed with plasmid expressing *S. pombe dbr1*$^+$ cDNA fused to the *GAL1* promoter on plasmid pRS316GU (strain YKN159-2, lanes 7 and 8). Transformed *dbr1* cells initially were grown overnight in minimal selective media (lanes 3–8) containing 2% raffinose as the sole carbon source. Cells were harvested, washed, and transferred to fresh selective media containing 2% glucose for repression or 2% galactose for induction of *C. elegans dbr-1*(+) (lane 6) and *S. pombe dbr1*$^+$ (lane 8) genes. Total RNA was isolated for RNA blot analysis 1–2 days after the medium shift. Each lane contained an equal amount of total RNA, and the blot was hybridized with a U24-specific probe. The small amount of mature U24 observed in lane 7 for the *S. pombe* construct suggests that the *S. pombe dbr1*$^+$ cDNA may be able to partially overcome glucose repression in *S. cerevisiae*.

tion in transformed cells during growth on glucose or galactose demonstrated that both heterologous *DBR1* genes can rescue the defect in intronic snoRNA production (Fig. 3). The complementation, however, appears to be incomplete. A similar situation was observed previously, when degradation of the actin mRNA intron was analyzed in *dbr1* cells expressing *DBR1* homologues from *S. pombe* or *C. elegans*. During the galactose induction period, even though cells were grown in selective medium, cells that lost the plasmid could still divide several times due to large internal pools of tryptophan or uracil (Nam et al., 1997). During this time period, we believe Dbr1p is rapidly lost, and introns reaccumulate. In summary, Dbr1p with diverse protein sequences can provide the debranching activity required for efficient intronic snoRNA biosynthesis.

Differential effect of *dbr1* mutation on production of intronic snoRNAs

Inspection of the snoRNA patterns from the *dbr1* strain revealed that loss of the debranching activity has differential effects on the synthesis of intronic snoRNAs (Fig. 2B; see also Petfalski et al., 1998). Processing of U24 and snR38 is almost completely blocked by the *dbr1* mutation; instead, snoRNAs trapped within the intron lariat accumulate. Processing of U18 and snR44 is also severely affected by *dbr1* mutation, however, mature snoRNAs can still be detected. In contrast, significant amounts of mature snR39 and snR59 snoRNAs are produced in the *dbr1* mutant. Most dramatically, only 20% of snR39 accumulates in the lariat form, whereas 80% occurs as mature snoRNA.

We noticed that the percentage of mature intronic snoRNA that accumulates in *dbr1* cells correlates strongly with the total length of the noncoding intron regions located between the 5′ splice site and branch point (Fig. 4). SnoRNAs encoded within longer introns are affected less severely by the *dbr1* mutation (Table 1). We propose that this correlation reflects endonucleolytic cleavages within the RNA lariat, which release the snoRNA from the intron trap. These cleavages could be random or pseudo-random, or might even be mediated by enzymes normally involved in maturation of snoRNA precursors [e.g., processing of a dicistronic snR190-U14 transcript in *S. cerevisiae* almost certainly involves cleavages by endonucleases (Petfalski et al., 1998)]. As observed in our analysis, larger lariats should be statistically more susceptible to

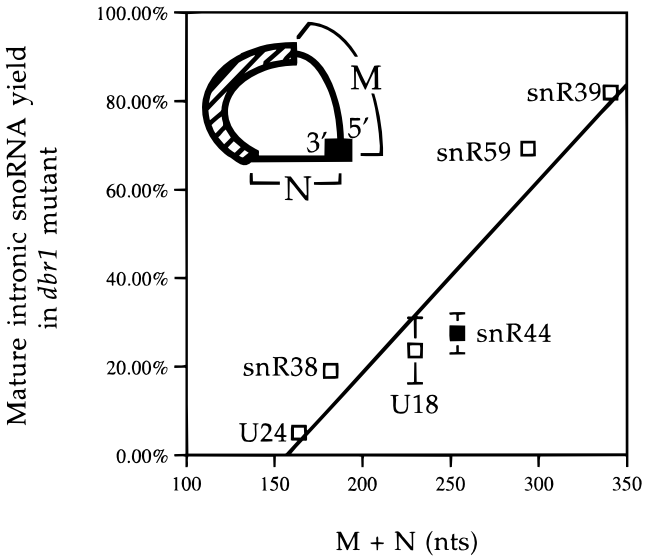

FIGURE 4. Differential effect of the *dbr1* mutation on intronic snoRNA biosynthesis. The plot depicts the relationship of intronic snoRNA production in *dbr1* cells and the size of the lariat. In particular, lariat size is given as the sum of the noncoding segments flanking the snoRNA, where M is the segment from the 5′ splice site to the 5′ end of the snoRNA, and N is the segment from the 3′ end of the snoRNA to the branch point. Mature intronic snoRNA yield is expressed as percent of tested intronic snoRNA that is in the mature form, where the total is the sum of mature and unprocessed snoRNA in both the intron lariat and linearized intron forms. Two different *dbr1* strains, KC99 and KC106 (see Table 1), were analyzed, and the results were averaged. Mean and standard deviations were plotted on the graph for all data points. Introns indicated by open rectangles encode the box C/D snoRNA species U24, snR38, U18, snR59, and snR39, listed by increasing intron length. Intron that encodes the snR44 box H/ACA intronic snoRNA is indicated by a closed rectangle.

TABLE 1. Effect of intron length on intronic snoRNA biosynthesis in *dbr1* mutant.

SnoRNA	Class	Host gene	SnoRNA size (nt)	Total intron size (nt)	M[a] (nt)	N[a] (nt)	Noncoding[a] intron size (M+N)	Mature intronic[a] snoRNA yield
U24	C/D	*BEL1*	89	273	79	85	164	5.1
snR38	C/D	*EF-1γ*	95	326	89	93	182	19.0
U18	C/D	*EF-1β*	102	366	113	117	230	23.6
snR44	H/ACA	*RP24*	211	483	134	120	254	27.5
snR59	C/D	*YL8B* (*RPL6B*)	78	407	161	133	294	69.3
snR39	C/D	*YL8A* (*RPL6A*)	89	461	181	160	341	82.0
pSO2-U24[b]	C/D	*BEL1*	89	273	79	85	164	2.7
pSO5-U24[b]	C/D	*BEL1*	89	429	235	85	320	9.2
pSO4-U24[b]	C/D	*BEL1*	89	562	368	85	453	30.6

[a]M, N, noncoding intron size, and mature intronic snoRNA yield are defined in the legend of Figure 4.
[b]pSO2-U24, pSO5-U24, and pSO4-U24 are the p*GAL1-BEL1/U24* constructs described in Figure 5A.

endonucleolytic cleavage and, hence, are better substrates for a Dbr1p-independent maturation pathway of intronic snoRNA. Following such cleavage, the linearized intron would undergo exonucleolytic processing to yield the mature-length snoRNA. It is not known whether 5′ → 3′ and 3′ → 5′ exonucleases can process through exposed branch points. If they can, then, in theory, one endonucleolytic cleavage would be sufficient to yield mature-length snoRNA.

Effect of intron length on production of a box C/D snoRNA in *dbr1* cells

To gain additional insight into the Dbr1p-independent maturation pathway, we tested directly the influence of intron length on intronic box C/D snoRNA synthesis in *dbr1* cells. Specifically, we examined production of the U24 box C/D snoRNA from introns of different length.

The U24 snoRNA of *S. cerevisiae* is normally encoded within the single intron of the *BEL1* gene, the mRNA of which encodes a G-beta-like protein. In our analysis, the full-length *BEL1/U24* transcription unit, containing the intron and U24 snoRNA, was fused to the *GAL1* promoter on a centromeric plasmid (construct pSO2; Fig. 5A). The native 273-nt host intron of U24 was lengthened to 429 and 562 nt by inserting 156- and 289-bp yeast DNA fragments between the 5′ splice donor and the U24 coding region (constructs pSO5 and pSO4, respectively). The inserts were derived from the intron of the *RP51A* gene, which encodes a ribosomal protein; this intron does not contain any snoRNA. These three p*GAL1-BEL1/U24* constructs were transformed into *DBR1 u24*Δ and *dbr1 u24*Δ cells. The chromosomal allele for U24 in these strains had been inactivated by replacement of the U24 coding segment with the *kanMX4* marker gene (Fig. 5B, see also Wach et al., 1994). Expression of the experimental p*GAL1-BEL1/U24* was then analyzed in transformants grown on galactose medium.

U24 snoRNA was efficiently processed into its mature form in *DBR1 u24*Δ cells, regardless of intron length (Fig. 5C, lanes 4–6). However, in comparison to the native length intron-encoded *BEL1/U24* gene, as the intron length increased, about 30% reduction in spliced *BEL1* mRNA was observed in both *DBR1 u24*Δ and *dbr1 u24*Δ strains (data not shown), correlating fairly well with the 40% reduction in mature U24 snoRNA production observed in *DBR1 u24*Δ strain. Presumably, lengthening of the introns resulted in less stable or less efficiently spliced *BEL1* pre-mRNA. In *dbr1 u24*Δ cells, increasing the length of the host intron for U24 to 429 and 562 nt had little effect on the raw amount of mature U24 (Fig. 5C, lanes 8–10). However, these apparent yields need to be corrected for the lower abundance of the *BEL1* mRNA that resulted from lengthening the intron. As the intron length increased, the percentage of mature U24 in the plasmid-containing *dbr1 u24*Δ cells relative to that of the corresponding plasmid-containing wild-type *DBR1 u24*Δ cells increased by twofold (Fig. 5C); a three- or fourfold increase was observed in an experiment in which the intron-containing fragment was inserted in the opposite orientation (not shown). Additionally, a decrease in the level of the U24 lariat form was also observed in *dbr1 u24*Δ cells as intron length increased. This effect could be caused by the decrease in splicing efficiency alone, or by increased endonucleolytic cleavage of the larger intron lariats. The fact that similar results were obtained when *RP51A* intron sequences were inserted into the U24 intron in the opposite orientation (not shown) supports the conclusion that primarily the length, and to a lesser extent, the sequence of the intron, determines the efficiency of U24 maturation. Taken together, these results argue that the efficiency of intronic snoRNA biosynthesis in *dbr1* cells depends primarily on the length of the intron encoding it.

Use of *dbr1* as a tool to determine whether a snoRNA is intronic or nonintronic

Our results show that synthesis of all known intronic snoRNAs is affected in *dbr1* cells: levels of mature

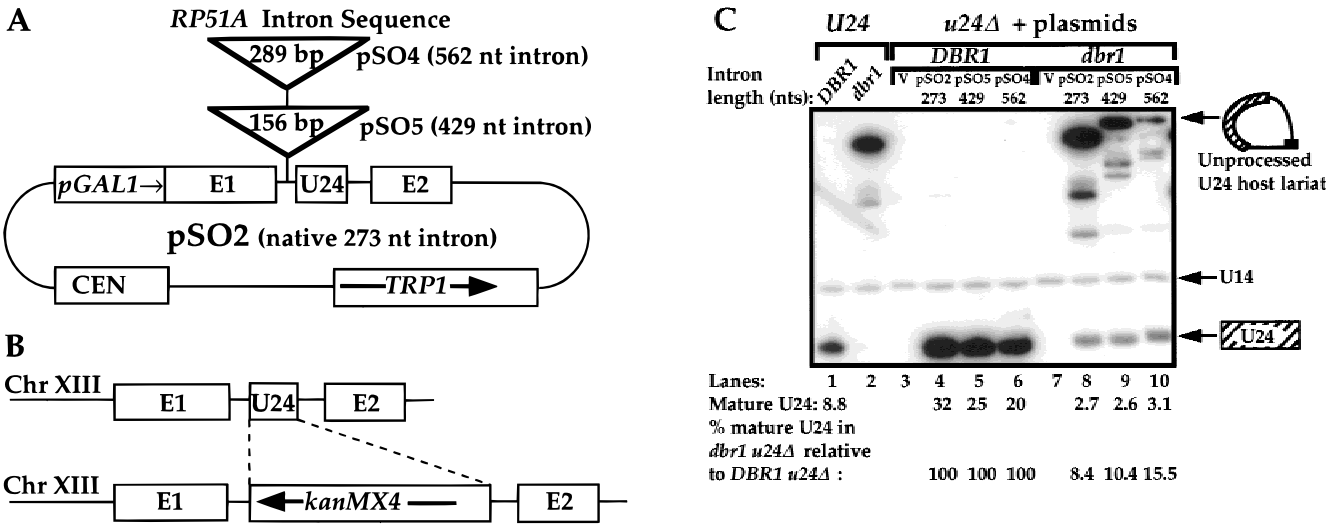

FIGURE 5. U24 biosynthesis in *dbr1* cells depends on intron length. **A:** Schematic diagram of the experimental p*GAL1-BEL1/U24* vectors. *BEL1/U24* expression is driven by the *GAL1* promoter. Fragments of 156 and 289 bp from the *RP51A* intron were cloned into plasmid pSO2, in a *Mam* I site within the *BEL1* intron, upstream of U24, to generate constructs pSO5 and pSO4, respectively. **B:** Strategy used to construct the *DBR1 u24*Δ strain. This strain was constructed by replacing the genomic segment that encodes U24 snoRNA with a *kanMX4* marker gene. Transcription orientation of the *kanMX4* gene is indicated by an arrow. *BEL1* mRNA is not expressed from this mutant allele, most likely because of insertion of the large 1.6-kb *kanMX4* DNA fragment into the *BEL1* intron. **C:** Analysis of U24 snoRNA accumulation in *DBR1* and *dbr1* cells. Total RNA was isolated from *DBR1* (strain YH8, lane 1), *dbr1* (strain KC99, lane 2), *DBR1 u24*Δ and *dbr1 u24*Δ cells transformed with vector pRS314GU alone (V; strains YSO35 and YSO39, lanes 3 and 7), vector expressing full-length *BEL1/U24* in its native 273-nt-long intron (pSO2; strains YSO36 and YSO40, lanes 4 and 8), vector expressing *BEL1/U24* in a 429-nt-long intron (pSO5; strains YSO37 and YSO41, lanes 5 and 9), and vector expressing *BEL1/U24* in a 562-nt-long intron (pSO4; strains YSO38 and YSO42, lanes 6 and 10). Transformed *DBR1 u24*Δ and *dbr1 u24*Δ cells were initially grown overnight in minimal selective media containing 2% raffinose as the sole carbon source. Cells were harvested, washed, and transferred to fresh selective media containing 2% galactose to induce *BEL1* expression. Total RNA was isolated for total RNA blot analysis using a U24-specific probe. Mature U24 values were normalized to the U14 levels. Mature U24 in *dbr1 u24*Δ cells was calculated as the percentage of mature U24 in the corresponding *DBR1 u24*Δ cells. Treatment of total *dbr1 u24*Δ RNA with recombinant His-tagged Dbr1p enzyme showed that the second slowest migrating band in lanes 8–10 is the linearized intron. Based on electrophoretic mobility, the third and fourth slowest migrating bands in lanes 8–10 correlate with 5′- and 3′-extended U24 variants, respectively. Mature intronic snoRNA yield (described in the legend of Fig. 4) for lanes 8–10 is listed in Table 1. *Saccharomyces* Genome Database ID number for *BEL1* gene is S0004722.

snoRNAs are reduced and precursors are trapped in the lariat structures. In contrast, production of all tested nonintronic snoRNAs is unaffected in *dbr1* cells. These results indicate that analysis of snoRNA accumulation patterns in *dbr1* cells can be a simple and reliable means to determine whether a specific snoRNA is of intronic or nonintronic origin.

To this end, we examined expression of several snoRNAs of unknown genomic status: the box C/D species snR40, snR41, snR47, and snR48, and a box H/ACA species snR36. No canonical *cis* splicing elements (i.e., 5′ and 3′ splice sites and branch point) can be found in the genomic vicinity of the coding sequences for these snoRNAs, which argues that they are nonintronic. On the other hand, all these snoRNAs lack a 5′ trimethylguanosine (TMG) cap structure, a feature common to intronic snoRNAs; polycistronic snoRNAs also lack 5′ caps (see also Discussion). Total RNA blot analysis showed that production of these five snoRNAs is insensitive to the *dbr1* mutation (Fig. 6). We conclude that these snoRNAs are not intronic.

Unprocessed intronic U24 snoRNA appears to function in 2′-*O*-methylation

In *S. cerevisiae*, the U24 intronic snoRNA directs 2′-*O*-methylation of 25S rRNA at residues C_{1436}, A_{1448}, and G_{1449} (Kiss-Laszlo et al., 1996, 1998). We asked whether U24 trapped within a lariat can still provide this function, by comparing the methylation patterns of 25S rRNA in *dbr1* and wild-type haploid cells. Methylation was analyzed by reverse transcription of the rRNA target regions. At low dNTP concentrations, reverse transcription pauses one nucleotide before a site of 2′-*O*-methylation (Maden et al., 1995).

When 25S rRNA from wild-type and *u24*Δ cells was analyzed, the expected patterns were seen: strong bands were observed corresponding to the sites of methylation governed by U24 from wild-type cells, but not from cells lacking U24 (Fig. 7C, lane 7 versus 13). Unexpectedly, strong pause bands were also observed at these three sites in rRNA from *dbr1* cells (Fig. 7C, lane 10). The band pattern for the *dbr1* rRNA was essentially indistinguishable from wild-type rRNA, indicat-

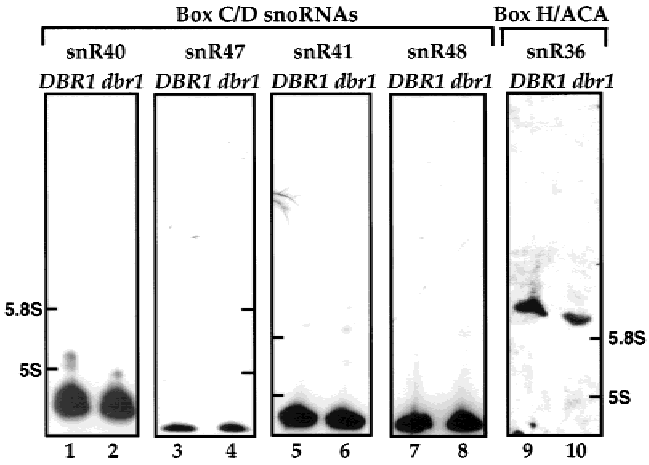

FIGURE 6. Expression of candidate intronic snoRNAs in the *dbr1* mutant. Total RNA was isolated from *S. cerevisiae DBR1* (strain YH8) and *dbr1* (strain KC99) cells, fractionated on gels of 10% (lanes 1–2) or 8% (lanes 3–10) polyacrylamide/8 M urea and total RNA blot analysis was performed as described in Materials and Methods. Probes were specific for *S. cerevisiae* snoRNAs whose intronic/nonintronic status had not been established. None of the snoRNAs examined accumulated in the lariat forms in *dbr1* cells, indicating that these snoRNAs are not intronic. GenBank accession numbers for the following snoRNAs are given in parentheses: snR40 (U26015); snR47 (U56648); snR41 (U26016); snR48 (AF064261); and snR36 (L33804).

ing that the *dbr1* mutation does not block methylation targeted by U24 snoRNA. In principle, this activity could be mediated by the residual amount of mature U24 in *dbr1* cells (estimated at 5% of the total U24 snoRNA in *dbr1* cells; Fig. 4), or by U24 in the lariat form.

To resolve this issue, we investigated whether the amount of residual mature U24 in *dbr1* cells is sufficient to fully methylate 25S rRNA at the three relevant positions. The full-length *BEL1/U24* transcription unit, containing the intron and U24, was fused to the weak *URA3* promoter in a centromeric plasmid (pSO3) and transformed into haploid *S. cerevisiae u24*Δ cells (Fig. 7A). The *u24*Δ transformants produce about twofold more mature U24 than *dbr1* cells (Fig. 7B, lanes 4 versus 2). When rRNA from the *u24*Δ cells transformed with p*URA3-BEL1/U24* was analyzed for methylation, the intensities of the bands at all three sites guided by U24 were reduced dramatically but not eliminated compared to those observed for rRNA from wild-type and *dbr1* cells (Fig. 7C, lanes 16 versus 7 and 10). Two strong pause bands at nonmethylated A1478 and G1479 sites were used as an internal quantitative control. Reverse transcriptase can also pause one nucleotide before certain nonmethylated residues, possibly as a result of the secondary structures of rRNA; this effect has been observed previously (Maden et al., 1995; Kiss-Laszlo et al., 1996). This result suggests that the residual amount of mature U24 in *dbr1* cells is not sufficient to fully methylate 25S pre-ribosomal rRNA at the sites normally served by this snoRNA.

To validate the quantitative difference observed in methylation, we analyzed the modification pattern of rRNA prepared from homozygous wild-type, *dbr1*, and *u24*Δ diploid cells. We reasoned that the quantitative methylation difference observed in haploid *u24*Δ cells would be enhanced in diploid *u24*Δ cells transformed with the p*URA3-BEL1/U24* single-copy centromeric plasmid, because the ratio of rRNA substrate to mature U24 would be larger. In other words, in comparison to the haploid cells, the total amount of rRNA should double in diploid *u24*Δ cells transformed with p*URA3-BEL1/U24*, whereas the amount of mature U24 should be almost constant because it is expressed from a single-copy centromeric plasmid. For the *dbr1* diploid cells, the amount of mature U24 should double, making the amount of mature U24 produced in both diploid *dbr1* and *u24*Δ cells transformed with p*URA3-BEL1/U24* almost equal. Indeed, diploid *u24*Δ cells transformed with p*URA3-BEL1/U24* produced about as much mature U24 as diploid *dbr1* cells (Fig. 7D, lane 4 versus 2).

The reverse transcription patterns showed that the extent of methylation at the three sites of interest was significantly reduced or eliminated in *u24*Δ cells transformed with p*URA3-BEL1/U24*, compared to rRNA from diploid wild-type and *dbr1* cells (Fig. 7E, lanes 16 versus 7 and 10). This result showed that the residual amount of mature U24 in *dbr1* cells is not sufficient to fully methylate 25S pre-rRNA at the three U24 sites.

In addition, when methylation in *dbr1 u24*Δ cells expressing p*URA3-BEL1/U24* was compared with *DBR1 u24*Δ expressing p*URA3-BEL1/U24*, in both haploid and diploid cells, the band patterns were indistinguishable (data not shown). Thus, even though the *dbr1* mutation affects U24 snoRNA processing, this mutation has no effect on rRNA methylation at the test sites. Methylation was correlated with the total amount of U24 present in cells rather than the maturation state. Taken together, these results strongly suggest that pre-U24 in the lariat form is functional.

DISCUSSION

Coding sequences for snoRNAs are found in several genomic arrangements (see Introduction). We analyzed the production of more than 15 intronic and nonintronic snoRNA species in a *S. cerevisiae* strain in which the lariat-debranching enzyme gene *DBR1* is disrupted. Our results demonstrate that Dbr1p, whose substrate, the intron lariat, is generated by pre-mRNA splicing, is required for proper biosynthesis of all known intronic snoRNAs, but not snoRNAs encoded in mono- or polycistronic transcription units. Indeed, in the *dbr1* mutant cells, immature forms of intronic snoRNAs start to accumulate, trapped within nondebranched intron lariats. Our data are in excellent agreement with results obtained recently with the U18 and U24 intronic

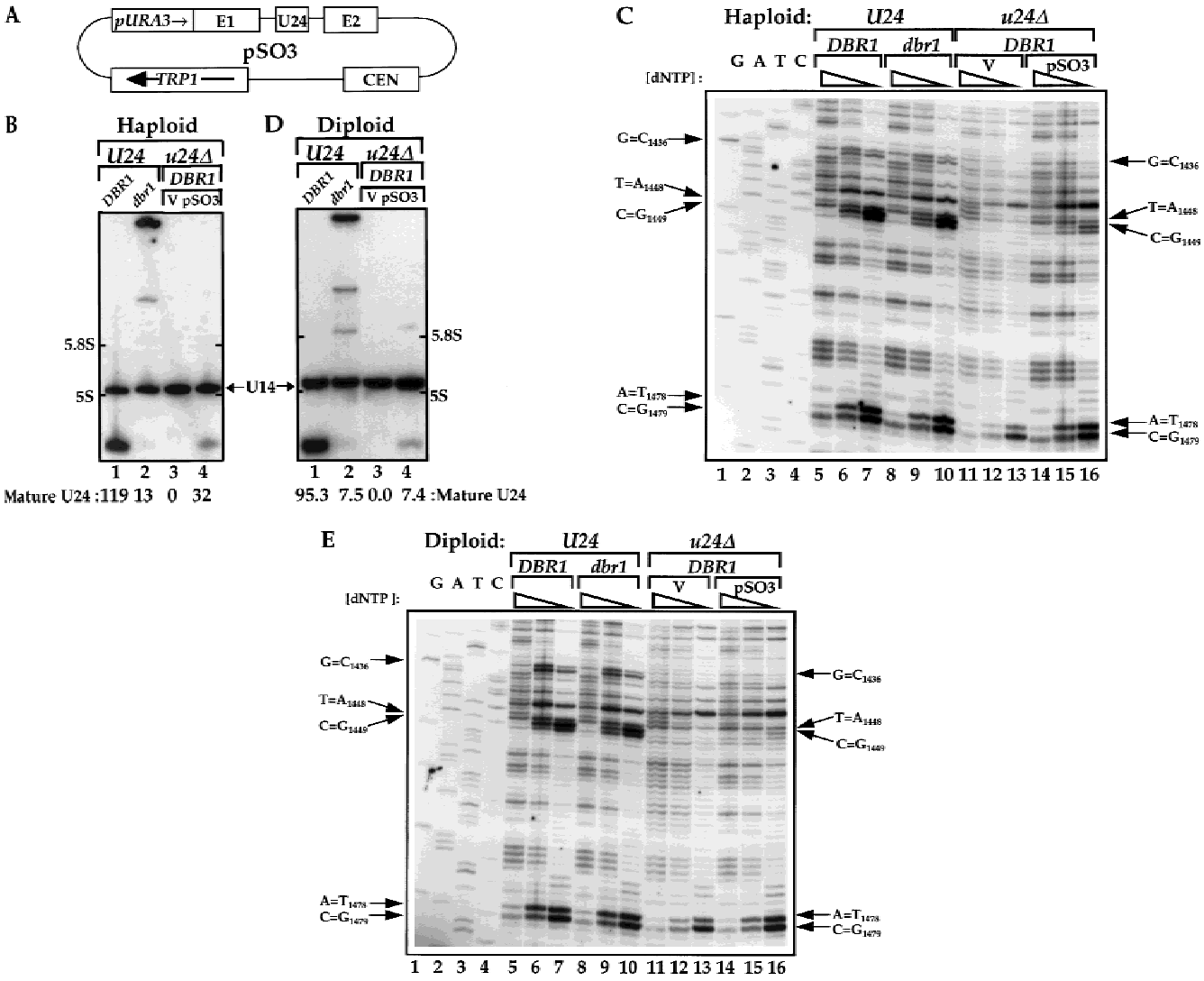

FIGURE 7. Unprocessed intronic U24 appears to direct 2′-*O*-methylation. **A:** Schematic diagram of p*URA3-BEL1/U24* vector pSO3. *BEL1/U24* expression is driven by the *URA3* promoter. **B:** Total RNA was isolated from haploid *DBR1 U24* (strain YH8, lane 1), *dbr1 U24* (strain KC99, lane 2), *DBR1 u24*Δ with vector pRS314GU alone (V; strain YSO35, lanes 3), and *DBR1 u24*Δ transformed with full-length *BEL1/U24* driven by the *URA3* promoter (strain YSO57, lanes 4). Transformed *DBR1 u24*Δ cells were grown in selective medium containing 2% glucose. Ten micrograms of total RNA was loaded in each lane, and hybridization was performed with a U24-specific probe. Values for mature U24 were normalized to control U14 levels. **C:** Primer extension analysis was performed using 5′ end ^{32}P-labeled gel-purified primer JB1878, with total RNAs isolated from: haploid *DBR1 U24* (strain YH8, lanes 5–7), *dbr1 U24* (strain KC99, lanes 8–10), *DBR1 u24*Δ transformed with vector pRS314GU alone (VA; strain YSO35, lanes 11–13), and *DBR1 u24*Δ transformed with full-length *BEL1/U24* driven by the *URA3* promoter (pSO3; strain YSO57, lanes 14–16). AMV reverse transcriptase was used with decreasing concentrations of dNTPs (200 μM, 4 μM, and 1 μM in lanes 5–7, 8–10, 11–13, and 14–16, respectively). 25S rDNA sequencing using dideoxynucleotides was performed using the same primer (lanes 1–4). **D:** Total RNA was isolated from homozygous diploids *DBR1 U24* (strain YSO49, lane 1), *dbr1 U24* (strain YSO50, lane 2), *DBR1 u24*Δ transformed with vector pRS314GU alone (V; strain YSO53, lane 3), and *DBR1 u24*Δ transformed with full-length *BEL1/U24* driven by the *URA3* promoter (pSO3; strain YSO54, lane 4). Transformed *DBR1 u24*Δ cells were grown in selective medium containing 2% glucose. Total RNA blot analysis and quantitation were performed as indicated in panel A. **E:** Primer extension analysis was performed as indicated in panel C using a 5′-end ^{32}P-labeled gel-purified primer JB1878 with total RNAs isolated from the following cells: homozygous diploid strains *DBR1 U24* (strain YSO49, lanes 5–7), *dbr1 U24* (strain YSO50, lanes 8–10), *DBR1 u24*Δ transformed with vector pRS314GU alone (VA; strain YSO53, lanes 11–13), and *DBR1 u24*Δ transformed with full-length *BEL1/U24* driven by the *URA3* promoter (pSO3; strain YSO54, lanes 14–16). The quantitative difference observed at rRNA methylation sites is due to changes in U24, not *BEL1* expression levels, because rRNA methylation at residues C_{1436}, A_{1448}, and G_{1449} is lost in both *BEL1 u24*Δ and *bel1*Δ *u24*Δ strains (data not shown).

snoRNAs examined in the same mutant strain (Petfalski et al., 1998). Together, these findings are consistent with the view that pre-mRNA splicing is a critical step in the biogenesis of intronic snoRNAs. However, for all intronic snoRNAs tested, some amount of mature RNA is still produced in the *dbr1* cells. This fact indicates that intronic snoRNAs can be produced in *S. cerevisiae* by a debranching enzyme-independent

pathway and thus suggest that a splicing-independent mechanism for intronic snoRNA production may exist.

Interestingly, the extent of accumulation of the snoRNA lariat precursor in *dbr1* cells varies among different snoRNAs. Similarly, different amounts of mature molecule can be detected for various intron-encoded snoRNAs. We noticed that the ratio of mature to total intronic snoRNA forms that accumulate in *dbr1* cells correlates with the length of the corresponding intron. Thus, snoRNAs encoded within shorter introns such as U24 and snR38 are affected more severely by the *dbr1* mutation, and accumulate much more unprocessed lariat snoRNAs than those encoded within longer introns, e.g., snR59 and snR39. This correlation suggests that "release" of snoRNA from the intron lariat "trap" in *dbr1* cells might occur as a result of endonucleolytic cleavage(s) inside the lariat. These cleavages could occur in a random or pseudo-random fashion or, perhaps, by enzymes normally involved in processing of nonintronic snoRNAs. In our model, the probability of these cleavages increases with the size of the lariat. In this scheme, only cleavages outside the snoRNA coding region can lead to a stable RNA product; cleavages inside the coding region lead to complete degradation of the lariat RNA (see Fig. 8). Remarkably, we found a strong correlation between the percent mature intronic snoRNA accumulated in *dbr1* mutant and the total length of the noncoding segments in the lariat. This relationship strongly supports our suggestion that mature intronic snoRNAs present in *dbr1* cells arise from random or pseudo-random cleavages of the intron by RNA endonucleases. Additional support comes from our demonstration that insertion of random DNA into the U24-containing intron positively affects conversion of RNA lariats into mature snoRNA in *dbr1* cells.

In addition to RNA species trapped in the lariat form, small amounts of snoRNAs extended at the 5′ end also accumulate in *dbr1* cells (Fig. 2D, lanes 2, 4, and 5). We suggest that these 5′-end extended snoRNAs also originate from random or pseudo-random endonucleolytic cleavage of intron lariats (see Fig. 8). If an intron lariat is cleaved upstream of the snoRNA segment, the 5′ noncoding region would be degraded rapidly by both 5′ → 3′ and 3′ → 5′ exonucleases, generating 3′-extended pre-snoRNA containing an exposed branch point that could, in principle, interfere with intron deg-

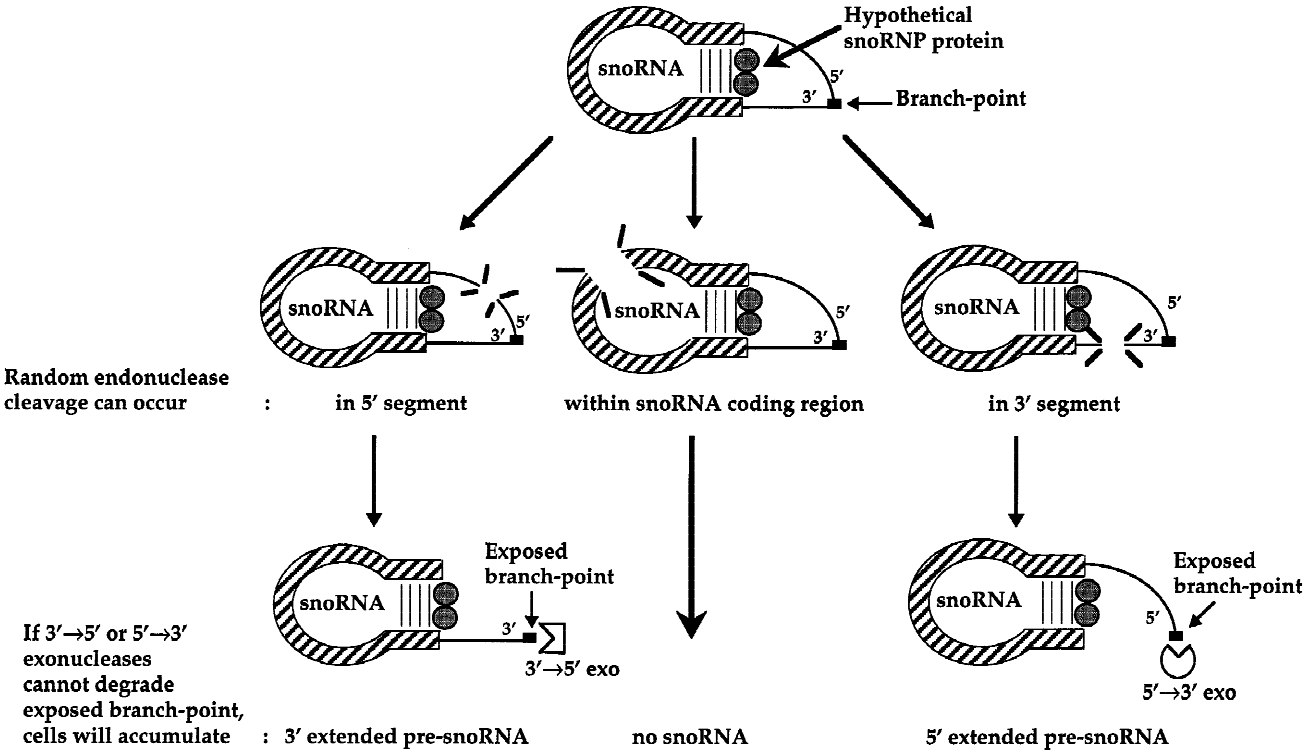

FIGURE 8. Model for how 5′-extended pre-snoRNA is generated in *dbr1* mutant. If an intron lariat pre-snoRNA is cleaved by a (pseudo)random endonuclease upstream of the snoRNA segment, the 5′ noncoding region would be degraded rapidly in opposite directions by both 3′ → 5′ and 5′ → 3′ exonucleases. Intronic snoRNA is assumed to be protected from degradation by the secondary structure of the snoRNA and snoRNP complex. If the 3′ → 5′ exonuclease cannot degrade the exposed branch point, 3′-extended pre-snoRNA should accumulate. Alternatively, if an intron lariat pre-snoRNA is cleaved downstream of the snoRNA, the reverse phenomenon may occur and 5′-extended pre-snoRNA should accumulate if the 5′ → 3′ exonuclease cannot degrade the exposed branch point. If random cleavage occurs within the snoRNA coding region, 3′ → 5′ and 5′ → 3′ exonucleases can degrade the entire snoRNA region rapidly, and no snoRNA will accumulate. 5′-Extended pre-snoRNA is observed in *dbr1* mutant cells, possibly because 3′ → 5′ exonuclease degrades exposed branch points more efficiently than 5′ → 3′ exonuclease.

radation by 3′ → 5′ exonuclease. It is not known whether 5′ → 3′ and 3′ → 5′ exonucleases can process through exposed branch points. Intronic snoRNA is assumed to be protected from degradation by the secondary structure of the snoRNA and the snoRNP complex. In contrast, if an intron lariat is cleaved downstream of the snoRNA coding region, the reverse phenomenon may occur and the exposed branch point in the 5′-extended region would interfere with 5′ → 3′ exonuclease activity, resulting in the accumulation of 5′-extended U24 pre-snoRNA. Only 5′-extended pre-snoRNA is observed in *dbr1* cells. In *dbr1 u24*Δ cells transformed with p*GAL1-BEL1/U24* (Fig. 4C, lanes 8–10), a third slowest-migrating band having the appropriate mobility for the 5′-extended pre-U24 snoRNA is observed. In addition, a faint band with the electrophoretic mobility that correlates well with 3′-extended pre-U24 snoRNA was also observed. However, we do not observe 3′-extended pre-snoRNA in the *dbr1* mutant, possibly because it does not exist or it exists at a very low level. This observation suggests that the 3′ → 5′ exonuclease(s) can degrade the exposed branch point more efficiently than 5′ → 3′ exonucleases. 5′-Extended snoRNA precursor has been shown to accumulate in the 5′ → 3′ exonuclease double mutant, *xrn1*-Δ,*rat1-1* (Petfalski et al., 1998). It will be interesting to determine whether Xrn1p and Rat1p can degrade exposed branch point RNA.

The positive complementation results obtained with the *C. elegans dbr-1*(+) and *S. pombe dbr1*$^+$ genes support the conclusion advanced earlier that the primary function of Dbr1p is to debranch excised intron lariats (Nam et al., 1997). The sequences of the *C. elegans* and *S. pombe* Dbr1p proteins are 33% and 40% identical to *S. cerevisiae* Dbr1p, respectively (Nam et al., 1997). It was demonstrated previously that these homologues can complement the intron accumulation defect in *dbr1* cells (Nam et al., 1997). Here, we showed that the *C. elegans* and *S. pombe* Dbr1p homologues also complement defects in intronic snoRNA biosynthesis. The growth rate of *S. cerevisiae dbr1* cells is slightly slower than that of wild-type cells, but a *S. pombe dbr1-1* mutant displays a severe growth defect (Nam et al., 1997). In *S. pombe*, it is possible that an intron-encoded RNA is necessary for growth, and that this is the basis of the requirement for the lariat-debranching activity.

Predicting whether a snoRNA is intronic or nonintronic is not a trivial task. Several criteria and combinations of criteria are used as indicators. The presence of a cap structure at the 5′ end of a mature snoRNA is a clear indication that the snoRNA is nonintronic. Absence of a cap indicates that 5′ end processing has occurred, but does not necessarily mean a snoRNA is intronic. In this regard, some snoRNAs, e.g., snR190 and U14, are apparently processed from a polycistronic transcript, by the combined action of endo- and exonucleases (Petfalski et al., 1998). The best predictor for an intronic snoRNA is the presence of canonical sequences for 5′ and 3′ splice sites, the splicing branch point, and flanking open reading frames of appropriate length. The absence of these components, however, does not disqualify a snoRNA as intronic. Noncapped snoRNAs derived from chromosomal regions without obvious exon/intron components are the most difficult to assign. The finding that production of intronic snoRNAs depends on the Dbr1p protein provides a simple and effective means of assaying for an intron coding arrangement. This is possible in *S. cerevisiae*, because cells lacking this enzyme (*dbr1*) are viable. We demonstrated that production of snoRNAs known to be nonintronic is not affected in the *dbr1* strain (Fig. 2A). In contrast, production of each intronic snoRNA tested is impaired in these cells (Fig. 2B). We also analyzed the production of five noncapped, candidate intronic snoRNAs, four box C/D snoRNAs (snR40, snR41, snR47, and snR48), and one box H/ACA snoRNA (snR36). All of these snoRNAs were expressed normally in the *dbr1* cells, indicating that none is encoded within an intron. Considering that *S. cerevisiae* may contain up to 100 different snoRNA species, of which less than 50 have been classified as intronic or nonintronic, the *dbr1* strain could become a valuable tool for classifying new snoRNAs.

Finally, our results indicate that U24 snoRNA in the lariat form can direct rRNA methylation. Specifically, three methylation sites in 25S rRNA that are served by U24 appear to be fully methylated in *dbr1* cells, even though mature U24 levels are down nearly 13-fold. In addition, the level of residual mature U24 present in the *dbr1* cells was determined to be insufficient to direct full methylation at these sites. Apparently, the lariat structure does not interfere with formation and activity of the U24 snoRNP complex. It would be interesting to investigate whether this situation holds true for other snoRNAs, such as the box H/ACA snoRNAs that have a more complex mode of recognizing rRNA substrates. In addition, rRNA methylation occurs in the nucleolus, whereas intronic snoRNA processing is thought to occur in the nucleoplasm. Thus, our results also strongly argue that U24 in the lariat form can efficiently access the nucleolus and, subsequently, the rRNA substrate.

SnoRNAs can be expressed either actively, from their own promoter, or passively, as part of a host intron of another gene. In mammals, several snoRNAs are encoded within different introns of the U22 host gene (*UHG*); and the resultant mRNA apparently does not encode any protein (Tycowski et al., 1996a). There is no obvious functional correlation between specific types of snoRNAs and the two modes of expression. Moreover, snoRNAs that are intronic in mammals, such as U14, are not necessarily so in yeast, and vice versa. This situation raises many questions about how snoRNAs become intron associated. An intriguing possibility is that placement within introns confers genomic

mobility on snoRNAs, or did so in the past. Because certain introns have been shown to be transposable via reverse splicing or reverse transcription (Zimmerly et al., 1995a, 1995b) and there are many other similarities between transposons and introns (Pret & Searles, 1991; Mueller et al., 1993), movement into introns could explain how snoRNAs have proliferated. Once duplicated, individual snoRNAs could have evolved new complementarities to rRNA and, if these improved fitness, they would be selected for. Thus, intronic snoRNAs may represent molecular fossils of an ancient radiation of function from a few ancestral snoRNAs (see also Smith & Steitz, 1997; Tollervey & Kiss, 1997).

MATERIALS AND METHODS

Strain constructions and growth media

The *S. cerevisiae* strains used in this study are described in Table 2. Unless stated otherwise, yeast strains were grown in rich media as described previously (Rose et al., 1990). All yeast strains were grown until the culture reached an A_{600} value of about 1.0. The yeast strains were transformed using the lithium acetate method (Schiestl & Gietz, 1989). Strains KC99 and KC106 (KM196 without plasmid pX3) were constructed as described previously (Chapman & Boeke, 1991). *DBR1 u24*Δ (YSO2-1) and *dbr1 u24*Δ (YSO3-1) mutant strains were constructed by gene replacement of the U24 coding region with the *kanMX4* marker (Wach et al., 1994), which confers dominant resistance to G418 (geneticin). The full-length *kanMX4* gene was amplified from the plasmid pRS400 (Brachmann et al., 1998) using oligonucleotide primers JB1774 and JB1775 (Table 3) containing the 5′ and 3′ sequences corresponding to those that flank the U24 coding region. The PCR product was transformed into *DBR1 U24* (YH8) and *dbr1 U24* (KC99) strains and transformants were selected on YPD plate containing 200 μg/mL of G418.

Plasmid constructions

All plasmids used are described in Table 4. Plasmids pSO2 and pSO3 were constructed as follows. Oligonucleotides JB1772 and JB1773 containing *Eco*R I sites were used to amplify the full-length *BEL1* gene in genomic DNA from the *DBR1 U24* (YH8) strain. The PCR product was digested with *Eco*R I and cloned into the *Eco*R I site of pRS314GU, a *S. cerevisiae* expression vector. pRS314GU is pRS314 with convergent *GAL1* and *URA3* promoter sequences cloned into the two opposite ends of the pRS314 polylinker site (Sikorski & Hieter, 1989; Nigro et al., 1992). The *BEL1* gene is driven by the *GAL1* promoter in plasmid pSO2 and by the *URA3* promoter in plasmid pSO3.

Plasmids pSO4 and pSO5 were constructed as follows. Oligonucleotides JB910 and JB911 were used to amplify the

TABLE 2. Strains used in this study.

Strain	Genotype	Plasmids	Parents
YH8	*MATα trp1Δ1 his3Δ200 leu2Δ1 ura3-167*		
KC99	*MATα trp1Δ1 his3Δ200 leu2Δ1 ura3-167 Δdbr1::HIS3*		YH8
KC106	*MATα trp1Δ1 his3Δ200 leu2Δ1 ura3-167 dbr1-1*		YH8
YKN120	*MATα trp1Δ1 his3Δ200 leu2Δ1 ura3-167 dbr1-1*	pKN107	KC106
YKN159-2	*MATα trp1Δ1 his3Δ200 leu2Δ1 ura3-167 dbr1-1*	pKN126	KC106
YSO2-1	*MATα trp1Δ1 his3Δ200 leu2Δ1 ura3-167 ΔU24::kanMX4*		YH8
YSO3-1	*MATα trp1Δ1 his3Δ200 leu2Δ1 ura3-167 ΔU24::kanMX4 Δdbr1::HIS3*		KC99
YSO35	*MATα trp1Δ1 his3Δ200 leu2Δ1 ura3-167 ΔU24::kanMX4*	pRS314GU	YSO2-1
YSO36	*MATα trp1Δ1 his3Δ200 leu2Δ1 ura3-167 ΔU24::kanMX4*	pSO2	YSO2-1
YSO37	*MATα trp1Δ1 his3Δ200 leu2Δ1 ura3-167 ΔU24::kanMX4*	pSO5	YSO2-1
YSO38	*MATα trp1Δ1 his3Δ200 leu2Δ1 ura3-167 ΔU24::kanMX4*	pSO4	YSO2-1
YSO39	*MATα trp1Δ1 his3Δ200 leu2Δ1 ura3-167 ΔU24::kanMX4 Δdbr1::HIS3*	pRS314GU	YSO3-1
YSO40	*MATα trp1Δ1 his3Δ200 leu2Δ1 ura3-167 ΔU24::kanMX4 Δdbr1::HIS3*	pSO2	YSO3-1
YSO41	*MATα trp1Δ1 his3Δ200 leu2Δ1 ura3-167 ΔU24::kanMX4 Δdbr1::HIS3*	pSO5	YSO3-1
YSO42	*MATα trp1Δ1 his3Δ200 leu2Δ1 ura3-167 ΔU24::kanMX4 Δdbr1::HIS3*	pSO4	YSO3-1
YSO49	*MAT**a** trp1Δ63 his3Δ200 leu2Δ1 ura3-167*		
	MATα trp1Δ1 his3Δ200 leu2Δ1 ura3-167		
YSO50	*MAT**a** trp1Δ1 his3Δ200 leu2Δ1 ura3-167 Δdbr1::HIS3*		
	MATα trp1Δ1 his3Δ200 leu2Δ1 ura3-167 Δdbr1::HIS3		
YSO53	*MAT**a** trp1Δ63 his3Δ200 leu2Δ1 ura3-167 ΔU24::kanMX4*	pRS314GU	
	MATα trp1Δ1 his3Δ200 leu2Δ1 ura3-167 ΔU24::kanMX4		
YSO54	*MAT**a** trp1Δ63 his3Δ200 leu2Δ1 ura3-167 ΔU24::kanMX4*	pSO3	
	MATα trp1Δ1 his3Δ200 leu2Δ1 ura3-167 ΔU24::kanMX4		
YSO55	*MAT**a** trp1Δ63 his3Δ200 leu2Δ1 ura3-167 ΔU24::kanMX4 Δdbr1::HIS3*	pRS314GU	
	MATα trp1Δ1 his3Δ200 leu2Δ1 ura3-167 ΔU24::kanMX4 Δdbr1::HIS3		
YSO56	*MAT**a** trp1Δ63 his3Δ200 leu2Δ1 ura3-167 ΔU24::kanMX4 Δdbr1::HIS3*	pSO3	
	MATα trp1Δ1 his3Δ200 leu2Δ1 ura3-167 ΔU24::kanMX4 Δdbr1::HIS3		
YSO57	*MATα trp1Δ1 his3Δ200 leu2Δ1 ura3-167 ΔU24::kanMX4*	pSO3	YSO2-1
YSO58	*MATα trp1Δ1 his3Δ200 leu2Δ1 ura3-167 ΔU24::kanMX4 Δdbr1::HIS3*	pSO3	YSO3-1

TABLE 3. Oligonucleotides used in this study.

Probes[a]	Name	Sequence[b]
U24	JB1591	GGTATGTCTCATTCGGAACTCAAAGTTCCATCTGAAGTAGC
snR38	JB1622	GAGAGGTTACCTATTATTACCCATTCAGACAGGGATAACTG
U18	JB1592	CTCTTTTGTCACTCATATCGGGGGTCTTACTTCCCATC
snR39	JB1623	CGACAGCATCGTCAATGACTAGTCGAATATGTATTGGG
snR59	JB1624	GGTGATTAAACGACAGCATTGTCAAAGACTAGTCGAG
snR44	JB1689	CCACATGGGATTAAATATCCCGGACAC
snR4	JB1594	CCTTCATAGGACACCTGAGTACTTGTGGCATCCATGTTCAG
snR13	JB1595	CCGTTACTGATTTGGCAAAAGCCAAACAGCAACTCGAGCC
snR45	JB1632	CAATGGGATGCGCAGGAACCGCTATCTCCATTAAAACCTCAG
snR190	JB1631	GTCACAGAAGCAACATCTTTTCAAAATCATTCGCATTAAGAG
U3b	JB1629	CCAAAGGAAGTTATCACAATTGCAACGGCAAAGC
U14	JB1630	CCGAGAGTACTAACGATGGGTTCGTAAGCGTACTCC
snR35	JB1690	GAACAAAATGATGATCTCTCCGATGGACTTGACGC
snR40	JB1593	CCTTCATAGGACACCTGAGTACTTGTGGCATCCATGTTCAG
snR41	JB1625	GGGTTGTCGACATGTAGTTAAACCACTATTCAGTCGG
snR47	JB1626	CCACCTATAAAGGATTCGGACGAAGAAATTCATG
snR48	JB1627	GGAGAGTACTTAAACTTCACATCCTAACATTAGAGATGCCAG
snR36	JB1691	CTCAAAGAAGTCTAATTGTTTTAGCCCGTTGATC
snR38 5′	JB1694	GACGTGCCAAATAAACGAACGGGAAACGCGC
snR38 3′	JB1695	CCTGGATTAGGACACGCTTTGTACTTCC
PE	JB1878	GAGCTTCCCCATCTCTTAGGATCGACTAAC
PCR	JB910	GTACGTATGTTAATATGGACTAAAGG
PCR	JB911	CCAGCTGTTAAAATGACGAAAAGCAATAC
PCR	JB1772	CGGAATTCATGGCATCTAACGAAGTTTTAG
PCR	JB1773	CGGAATTCTTAGTTAGCAGTCATAACTTGCC
PCR	JB1774	AATCGAGTAGAAGAAGAAAAGTGGATTTGTGTATGCCATGATTGTACTGAGAGTGCACC
PCR	JB1775	CATAACGAGTAAAGAGAAGAGCAGAGTAATGCTAAACCACTGTGCGGTATTTCACACCG

[a]Oligonucleotides used as PCR primers are designated PCR; primer extension oligonucleotide is designated PE.
[b]*Eco*R I restriction enzyme sites are underlined.

S. cerevisiae RP51A intron, using plasmid pHZ18 (Teem & Rosbash, 1983) as template. For construction of plasmid pSO4, the PCR product was digested with *Bsa*A I and *Eco*R V to generate a 289-bp fragment and cloned into the *Mam* I site of plasmid pSO2, within the *BEL1* intron, upstream of the U24 coding region. The pSO5 plasmid was constructed with the same PCR product, digested with *Bsa*A I and *Bst*X I, blunt-ended with T4 DNA polymerase to generate a 156-bp fragment, and cloned into the same *Mam* I site in pSO2. pKN107 is a plasmid with *C. elegans dbr-1*(+) cDNA cloned into pRS314GU (Nam et al., 1997), and pKN126 is a plasmid with *S. pombe dbr1*$^+$ cDNA cloned into pRS316GU (K. Nam & J.D. Boeke, unpubl. data).

Total RNA isolation and blotting analysis

Total yeast RNA was prepared by a standard hot acidic phenol extraction method (Collart & Oliviero, 1993). Ten to 30 μg of total RNA were fractionated on an 8% polyacrylamide/8 M urea gel, and subsequently transferred to a GeneScreen Plus nylon membrane (NEN Life Science Products) using an electro-blotter (Hoefer) with 1× MOPS buffer. RNA was cross-linked to the filter by UV irradiation in a Stratalinker (Stratagene) and total RNA hybridization analysis was performed with ^{32}P-labeled oligonucleotide probe(s) as described previously (Brown, 1993). Filters were washed in 0.2× SSC/0.1% SDS at 42 °C twice for 30 min. Quantitation was

TABLE 4. Plasmids used in this study.

Plasmid	Descriptions	Markers	References
pRS314GU	*S. cerevisiae* expression vector	*TRP1*	Sikorski & Hieter (1989)
pRS316GU	*S. cerevisiae* expression vector	*URA3*	Sikorski & Hieter (1989)
pKN107	*C. elegans-DBR1* cDNA driven by *GAL1* promoter in pRS314GU	*TRP1*	Nam et al. (1997)
pKN126	*S. pombe–DBR1* cDNA driven by *GAL1* promoter in pRS316GU	*URA3*	K. Nam & J.D. Boeke (unpubl.)
pSO2	Full-length *BEL1* DNA driven by *GAL1* promoter in pRS314GU	*TRP1*	This work
pSO3	Full-length *BEL1* DNA driven by *URA3* promoter in pRS314GU	*TRP1*	This work
pSO4	Full-length *BEL1* DNA inserted with a 289 bp *RP51A* intron fragment within its intron, driven by *GAL1* promoter in pRS314GU	*TRP1*	This work
pSO5	Full-length *BEL1* DNA inserted with a 156 bp *RP51A* intron fragment within its intron, driven by *GAL1* promoter in pRS314GU	*TRP1*	This work

performed using a phosphorimager (Molecular Dynamics) and ImageQuant (Molecular Dynamics) software.

Deoxyoligonucleotides probes used in the study are described in Table 3. The U24-specific probe is deoxyoligonucleotide JB1591. SnoRNA-specific probes were 5′ end-labeled with T4 polynucleotide kinase (NEB) and [γ-^{32}P]-ATP for 1 h, under reaction conditions described by the manufacturer. Before adding to the hybridization solution, labeled primers were purified from unincorporated [γ-^{32}P]-ATP using Centriflex gel filtration cartridge (Edge BioSystems, Inc.).

In vitro debranching of total RNA with Dbr1p protein

Ten micrograms of total RNA from *dbr1* (KC99) cells were treated with 0 ng, 46 ng, 140 ng, or 465 ng recombinant His-tagged Dbr1p protein in a 15-μL reaction mixture containing 20 mM HEPES/KOH, pH 7.6, 125 mM KCl, 0.5 mM $MgCl_2$, 1 mM DTT, and 10% glycerol for 30 min at 30 °C. The reaction was stopped by quenching on ice and adding an equal volume of stop solution containing 20 mM EDTA, 95% formamide, 0.05% bromophenol blue, and 0.05% xylene cyanol. Total RNA hybridization analysis was performed with a U24-specific probe (JB1591). Total RNA from *DBR1* (YH8) cells was used in control experiments.

Mapping rRNA methylations by primer extension analysis

About 2 pmol of 5′-end ^{32}P-labeled gel-purified primer JB1878 was annealed to 2 μg of yeast total RNA at 67 °C for 3 min, followed by incubation at 37 °C for 5 min. Primer extension was performed in a 10-μL reaction mixture containing 50 mM Tris-HCl, pH 8.5, 8 mM $MgCl_2$, 30 mM KCl, 1 mM dithiothreitol, with 0.5 μL of 25 U/μL AMV reverse transcriptase (Boehringer Manheim), and at 200 μM, 4 μM, and 1 μM final concentration of dNTPs at 37 °C for 30 min. Reaction products were then incubated in a solution containing 1 N NaOH and 12.5 mM EDTA, pH 8.0, at 95 °C for 5 min to degrade the RNA template, and then neutralized by adding 0.5 volume of 1 N HCl. After precipitation with ethanol, the reaction products were resuspended in 5 μL of 1× TE buffer, followed by the addition of 5 μL of stop solution containing 20 mM EDTA, 95% formamide, 0.05% bromophenol blue, and 0.05% xylene cyanol. Reaction products were then heated at 100 °C for 2 min, set on ice, and resolved on a 6% polyacrylamide/8 M urea gel. The control sequencing reaction was performed on plasmid carrying 25S rDNA sequence using the same 5′-end ^{32}P-labeled gel-purified primer according to the manufacturer's specifications (USB-Amersham).

ACKNOWLEDGMENTS

We thank members of the Boeke and Fournier laboratories for helpful discussions and for providing yeast strains. We also thank Joan Steitz for her role as catalyst and matchmaker; Kiebang Nam for supplying the pKN126 plasmid; Yolanda Eby for assistance with DNA sequencing; Charles Dann for providing Dbr1p enzyme, Jeff Smith for valuable advice and discussions, and George Brush, Greg J. Cost, Scott Devine, and Siyuan Le for critical reading of the manuscript. Supported by NIH grant GM36481 to J.D.B. and NSF grant MCB-9419007 to M.J.F.

Received May 15, 1998; returned for revision June 8, 1998; revised manuscript received June 11, 1998

REFERENCES

Bachellerie JP, Cavaille J. 1997. Guiding ribose methylation of rRNA. *Trends Biochem Sci 22*:257–261.

Balakin AG, Smith L, Fournier MJ. 1996. The RNA world of the nucleolus: Two major families of small RNAs defined by different box elements with related functions. *Cell 86*:823–834.

Bortolin ML, Kiss T. 1998. Human U19 intron-encoded snoRNA is processed from a long primary transcript that possesses little potential for protein coding. *RNA 4*:445–453.

Brachmann CB, Davies A, Cost GJ, Caputo E, Li J, Hieter P, Boeke JD. 1998. Designer deletion strains derived from *Saccharomyces cerevisiae* S288C: A useful set of strains and plasmids for PCR-mediated gene disruptions and other applications. *Yeast 14*:115–132.

Brown T. 1993. Analysis of RNA by Northern and slot blot hybridization. In: Ausubel FM, Brent R, Kingston RE, Moore DD, Seidman JG, Smith JA, Struhl K, eds. *Current protocols in molecular biology*. New York: John Wiley & Sons, Inc. pp 4.9.1–4.9.14.

Caffarelli E, Arese M, Santoro B, Fragapane P, Bozzoni I. 1994. In vitro study of processing of the intron-encoded U16 small nucleolar RNA in *Xenopus laevis*. *Mol Cell Biol 14*:2966–2974.

Caffarelli E, Fatica A, Prislei S, De Gregorio E, Fragapane P, Bozzoni I. 1996. Processing of the intron-encoded U16 and U18 snoRNAs: The conserved C and D boxes control both the processing reaction and the stability of the mature snoRNA. *EMBO J 15*:1121–1131.

Cavaille J, Bachellerie JP. 1996. Processing of fibrillarin-associated snoRNAs from pre-mRNA introns: An exonucleolytic process exclusively directed by the common stem-box terminal structure. *Biochimie 78*:443–456.

Cavaille J, Nicoloso M, Bachellerie JP. 1996. Targeted ribose methylation of RNA in vivo directed by tailored antisense RNA guides. *Nature 383*:732–735.

Cecconi F, Mariottini P, Amaldi F. 1995. The *Xenopus* intron-encoded U17 snoRNA is produced by exonucleolytic processing of its precursor in oocytes. *Nucleic Acids Res 23*:4670–4676.

Chapman KB, Boeke JD. 1991. Isolation and characterization of the gene encoding yeast debranching enzyme. *Cell 65*:483–492.

Collart MA, Oliviero S. 1993. Preparation of yeast RNA. In: Ausubel FM, Brent R, Kingston RE, Moore DD, Seidman JG, Smith JA, Struhl K. *Current protocols in molecular biology*. New York: John Wiley & Sons, Inc. pp 13.12.1–13.12.5.

Fragapane P, Prislei S, Michienzi A, Caffarelli E, Bozzoni I. 1993. A novel small nucleolar RNA (U16) is encoded inside a ribosomal protein intron and originates by processing of the pre-mRNA. *EMBO J 12*:2921–2928.

Ganot P, Bortolin ML, Kiss T. 1997a. Site-specific pseudouridine formation in preribosomal RNA is guided by small nucleolar RNAs. *Cell 89*:799–809.

Ganot P, Caizergues-Ferrer M, Kiss T. 1997b. The family of box ACA small nucleolar RNAs is defined by an evolutionarily conserved secondary structure and ubiquitous sequence elements essential for RNA accumulation. *Genes & Dev 11*:941–956.

Kiss-Laszlo Z, Henry Y, Bachellerie JP, Caizergues-Ferrer M, Kiss T. 1996. Site-specific ribose methylation of preribosomal RNA: A novel function for small nucleolar RNAs. *Cell 85*:1077–1088.

Kiss-Laszlo Z, Henry Y, Kiss T. 1998. Sequence and structural elements of methylation guide snoRNAs essential for site-specific ribose methylation of pre-rRNA. *EMBO J 17*:797–807.

Kiss T, Filipowicz W. 1995. Exonucleolytic processing of small nucleolar RNAs from pre-mRNA introns. *Genes & Dev 9*:1411–1424.

Leader DJ, Clark GP, Watters J, Beven AF, Shaw PJ, Brown JW. 1997. Clusters of multiple different small nucleolar RNA genes in plants are expressed as and processed from polycistronic pre-snoRNAs. *EMBO J 16*:5742–5751.

Leader DJ, Sanders JF, Waugh R, Shaw P, Brown JW. 1994. Molecular characterisation of plant U14 small nucleolar RNA genes: Closely linked genes are transcribed as polycistronic U14 transcripts. *Nucleic Acids Res 22*:5196–5203.

Maden BE, Corbett ME, Heeney PA, Pugh K, Ajuh PM. 1995. Classical and novel approaches to the detection and localization of the numerous modified nucleotides in eukaryotic ribosomal RNA. *Biochimie 77*:22–29.

Maxwell ES, Fournier MJ. 1995. The small nucleolar RNAs. *Annu Rev Biochem 64*:897–934.

Mueller MW, Allmaier M, Eskes R, Schweyen RJ. 1993. Transposition of group II intron *aI1* in yeast and invasion of mitochondrial genes at new locations. *Nature 366*:174–176.

Nam K, Hudson RH, Chapman KB, Ganeshan K, Damha MJ, Boeke JD. 1994. Yeast lariat debranching enzyme. Substrate and sequence specificity. *J Biol Chem 269*:20613–20621.

Nam K, Lee G, Trambley J, Devine SE, Boeke JD. 1997. Severe growth defect in a *Schizosaccharomyces pombe* mutant defective in intron lariat degradation. *Mol Cell Biol 17*:809–818.

Ni J, Tien AL, Fournier MJ. 1997. Small nucleolar RNAs direct site-specific synthesis of pseudouridine in ribosomal RNA. *Cell 89*:565–573.

Nigro JM, Sikorski R, Reed SI, Vogelstein B. 1992. Human p53 and CDC2Hs genes combine to inhibit the proliferation of *Saccharomyces cerevisiae*. *Mol Cell Biol 12*:1357–1365.

Petfalski E, Dandekar T, Henry Y, Tollervey D. 1998. Processing of the precursors to small nucleolar RNAs and rRNAs requires common components. *Mol Cell Biol 18*:1181–1189.

Pret AM, Searles LL. 1991. Splicing of retrotransposon insertions from transcripts of the *Drosophila melanogaster vermilion* gene in a revertant. *Genetics 129*:1137–1145.

Prislei S, Fatica A, De Gregorio E, Arese M, Fragapane P, Caffarelli E, Presutti C, Bozzoni I. 1995. Self-cleaving motifs are found in close proximity to the sites utilized for U16 snoRNA processing. *Gene 163*:221–226.

Prislei S, Michienzi A, Presutti C, Fragapane P, Bozzoni I. 1993. Two different snoRNAs are encoded in introns of amphibian and human L1 ribosomal protein genes. *Nucleic Acids Res 21*:5824–5830.

Rose MD, Winston F, Hieter P. 1990. *Methods in yeast genetics. A laboratory course manual*. Cold Spring Harbor, New York: Cold Spring Harbor Laboratory Press.

Samarksy DA, Fournier MJ, Singer RH, Bertrand E. 1998. The snoRNA box C/D motif directs nucleolar targeting and also couples snoRNA synthesis and localization. *EMBO J 17*:3747–3757.

Schiestl RH, Gietz RD. 1989. High efficiency transformation of intact yeast cells using single stranded nucleic acids as a carrier. *Curr Genet 16*:339–346.

Sikorski RS, Hieter P. 1989. A system of shuttle vectors and yeast host strains designed for efficient manipulation of DNA in *Saccharomyces cerevisiae*. *Genetics 122*:19–27.

Smith CM, Steitz JA. 1997. Sno storm in the nucleolus: New roles for myriad small RNPs. *Cell 89*:669–672.

Teem JL, Rosbash M. 1983. Expression of a beta-galactosidase gene containing the ribosomal protein 51 intron is sensitive to the *rna2* mutation of yeast. *Proc Natl Acad Sci USA 80*:4403–4407.

Tollervey D, Kiss T. 1997. Function and synthesis of small nucleolar RNAs. *Curr Opin Cell Biol 9*:337–342.

Tycowski KT, Shu MD, Steitz JA. 1996a. A mammalian gene with introns instead of exons generating stable RNA products. *Nature 379*:464–466.

Tycowski KT, Smith CM, Shu MD, Steitz JA. 1996b. A small nucleolar RNA requirement for site-specific ribose methylation of rRNA in *Xenopus*. *Proc Natl Acad Sci USA 93*:14480–11485.

Wach A, Brachat A, Pohlmann R, Philippsen P. 1994. New heterologous modules for classical or PCR-based gene disruptions in *Saccharomyces cerevisiae*. *Yeast 10*:1793–1808.

Watkins NJ, Leverette RD, Xia L, Andrews MT, Maxwell ES. 1996. Elements essential for processing intronic U14 snoRNA are located at the termini of the mature snoRNA sequence and include conserved nucleotide boxes C and D. *RNA 2*:118–133.

Zimmerly S, Guo H, Eskes R, Yang J, Perlman PS, Lambowitz AM. 1995a. A group II intron RNA is a catalytic component of a DNA endonuclease involved in intron mobility. *Cell 83*:529–538.

Zimmerly S, Guo H, Perlman PS, Lambowitz AM. 1995b. Group II intron mobility occurs by target DNA-primed reverse transcription. *Cell 82*:545–554.